Reference: *Biol. Bull.* **203:** 14–26. (August 2002)

Ontogeny of Squid Mantle Function: Changes in the Mechanics of Escape-Jet Locomotion in the Oval Squid, *Sepioteuthis lessoniana* Lesson, 1830

JOSEPH T. THOMPSON* AND WILLIAM M. KIER

Department of Biology, CB#3280 Coker Hall, University of North Carolina, Chapel Hill, North Carolina 27599-3280

Abstract. In *Sepioteuthis lessoniana*, the oval squid, ontogenetic changes in the kinematics of the mantle during escape-jet locomotion imply a decline in the relative mass flux of the escape jet and may affect the peak weight-specific thrust of the escape jet. To examine the relationship between ontogenetic changes in the kinematics of the mantle and the thrust generated during the escape jet, we simultaneously measured the peak thrust and the kinematics of the mantle of squid tethered to a force transducer. We tested an ontogenetic series of *S. lessoniana* that ranged in size from 5 to 40 mm dorsal mantle length (DML). In newly hatched squids, thrust peaked 40 ms after the start of the escape jet and reached a maximum of between 0.10 mN and 0.80 mN. In the largest animals, thrust peaked 70 ms after the start of the escape jet and reached a maximum of between 18 mN and 110 mN. Peak thrust was normalized by the wet weight of the squid and also by the cross-sectional area of the circumferential muscle that provides power for the escape jet. The weight-specific peak thrust of the escape jet averaged 0.36 in newly hatched squid and increased significantly to an average of 1.5 in the largest squids measured ($P < 0.01$). The thrust per unit area of circumferential muscle averaged 0.25 mN/mm^2 in hatchlings and increased significantly to an average of 1.4 mN/mm^2 in the largest animals tested ($P < 0.01$). The impulse of the escape jet was also lowest in newly hatched individuals (1.3 mN · s) and increased significantly to 1000 mN · s in the largest squids measured ($P < 0.01$). These ontogenetic changes in the mechanics of the escape jet suggest (1) that propulsion efficiency of the exhalant phase of the jet is highest in hatchlings, and (2) that the mechanics of the circumferential muscles of the mantle change during growth.

Received 25 July 2001; accepted 30 May 2002.

* To whom correspondence should be addressed. E-mail: joethomp@email.unc.edu

Abbreviation: DML, dorsal mantle length.

Introduction

The kinematics and mechanics of locomotion change significantly during the growth of many aquatic animals, especially in those that are small at hatching and grow to large body size. The ontogeny of the kinematics and mechanics of locomotion may reflect a change in the hydrodynamic environment of the animal as it grows (Weihs, 1974; Batty, 1984; Webb and Weihs, 1986; Osse, 1990; Williams, 1994; Müller and Videler, 1996). The size of the animal or its propulsor, the speed of the animal or its propulsor, and the kinematic viscosity of water all affect the forces experienced by an aquatic animal (*e.g.*, Lighthill, 1975). The Reynolds number (Re) describes the relationship among these three factors,

$$\mathrm{Re} = lU/\nu \qquad \text{(Lighthill, 1975)} \qquad \text{(Eq. 1)}$$

where l is a characteristic length of the organism (*e.g.*, body or propulsor length), U is the velocity of the organism (or a portion of the organism) relative to the surrounding water, and ν is the kinematic viscosity of the fluid (*i.e.*, the ratio of water viscosity to water density). The Reynolds number characterizes the relative importance of inertial forces and viscous forces on the swimming animal (Vogel, 1994). Thus, when the Reynolds number is high ($>10^3$), inertial forces dominate locomotion; when the Reynolds number is low (<1), viscosity dominates. In an intermediate Reynolds number fluid regime ($1 < \mathrm{Re} < 10^3$), inertial forces dom-

inate, but the effects of viscosity are considerable (Daniel *et al.*, 1992).

The hydrodynamic environment influences the mechanics of locomotion during ontogeny. For example, newly hatched larval brine shrimp and fish swim in a fluid regime between Re = 1 and Re = 20 (Batty, 1984; Williams, 1994; Müller *et al.*, 2000), where inertial and viscous forces are nearly equal. In such a hydrodynamic environment, inertial modes of locomotion, such as burst-and-coast swimming, are hypothesized to be energetically costly compared with drag-based modes of locomotion, such as steady anguilliform swimming (Weihs, 1974; Müller *et al.*, 2000). Thus, hydrodynamic considerations may explain the observed change from drag-based to inertial locomotion during the growth of larval brine shrimp and fish (Batty, 1984; Williams, 1994; Müller *et al.*, 2000).

Locomotion in some animals may be fixed, despite shifts in their hydrodynamic regime during growth. For example, the jet propulsion used by squids is analogous to the inertia-dependent burst-and-coast swimming employed by some fish. A squid produces a burst of thrust as the mantle contracts and expels water from the mantle cavity, followed by a coasting phase as the mantle expands and the mantle cavity refills. Because squids are limited to inertia-dependent jet propulsion for rapid swimming, the mechanics and energetics of locomotion for small hatchling squids may be compromised given the near parity of inertia and viscosity of their intermediate Re fluid environment ($1 < Re < 100$, unpub. obs. of *Sepioteuthis lessoniana* during fast and slow jetting). For instance, unlike adults, newly hatched individuals of *S. lessoniana* (unpub. obs.) and *Loligo vulgaris* (Packard, 1969) coast only a short distance after a burst of thrust. Because inertia-based modes of locomotion are unfavorable in the hydrodynamic environment of the hatchlings (Müller *et al.*, 2000), we might expect compensatory changes in the kinematics of the mantle and the mechanics of jet locomotion as squid grow.

Indeed, the amplitude of mantle movement during jet locomotion changes as a squid grows. In *Loligo vulgaris* (Packard, 1969), *L. opalescens* (Gilly *et al.*, 1991; Preuss *et al.*, 1997), and *S. lessoniana* (Thompson and Kier, 2001a), the maximum amplitude of mantle movement during the escape jet decreases dramatically during ontogeny. In *S. lessoniana*, the maximum contraction and hyperinflation of the mantle (both measured as the percent change from the resting mantle diameter) are significantly greater during an escape jet in small hatchlings than in the larger animals (Thompson and Kier, 2001a). The maximum contraction and hyperinflation of the mantle decrease exponentially until the squid reach a dorsal mantle length (DML) of about 15 mm. In squids larger than 15 mm DML, the maximum contraction and hyperinflation of the mantle during the escape jet remain unchanged (Thompson and Kier, 2001a). In addition, the maximum rate of contraction of the mantle during the escape jet is highest in hatchling squids and decreases exponentially until the animals reach 15 mm DML. In *S. lessoniana* specimens larger than 15 mm DML, the maximum rate of contraction of the mantle does not change significantly (Thompson and Kier, 2001a).

Specific problem. The ontogenetic changes in the kinematics of the mantle in *S. lessoniana* may affect the performance and the mechanical efficiency of escape-jet locomotion. Specifically, changes in the kinematics of the mantle result in higher relative mass flux (= mass of water exiting the mantle cavity per unit time, relative to body mass) in newly hatched squids than in larger animals (Thompson and Kier, 2001a). Because the thrust produced during the escape jet is proportional to the product of mass flux and the velocity of water exiting the funnel aperture (averaged over the funnel aperture; Vogel, 1994), a change in the relative mass flux may affect the thrust generated during the escape jet.

To explore how changes in the kinematics of the mantle impact escape-jet locomotion, we measured the peak thrust generated during the escape jet in an ontogenetic series of *S. lessoniana*. We examined the implications of an ontogenetic change in jet thrust on the propulsion efficiency of escape-jet locomotion, and on the mechanics of the circumferential muscles that power the jet. We also discuss the possibility that the evolution of ontogenetic changes in the morphology and kinematics of the mantle and funnel might reflect the scale effects of jet locomotion.

Materials and Methods

Animals

We obtained an ontogenetic series of *Sepioteuthis lessoniana* Lesson, 1830, the oval squid. Wild embryos collected from Izo, Japan, in September 1999 and August 2000 were raised by the National Resource Center for Cephalopods (NRCC) at the University of Texas Medical Branch, Galveston, Texas. The cohort consisted of thousands of embryos from six to eight different egg mops. Thus, it is likely that the sample populations were not the offspring of a few closely related individuals, but were representative of the natural population at the collection site.

The embryos were transported from the field to the NRCC and reared (Lee *et al.*, 1994). Commencing at hatching and at regular intervals thereafter, live squid were sent *via* overnight express shipping from the NRCC to the University of North Carolina. The squids ranged in size from 5 to 40 mm dorsal mantle length (DML) and in age from newly hatched to 6 weeks after hatching.

Prior to the start of the experiments, the animals were allowed at least 30 min to equilibrate in an 80-l circular holding tank. The temperature (23 °C) and salinity (35 ppt) of the water matched the temperature and salinity of the water in which the squid were raised. Circular water flow in the tank helped keep the squid swimming parallel to the

sides of the tank to prevent injury. No animal remained in the holding tank for longer than 2 h.

Every animal used for the experiments was in excellent condition. The coloration and activity of the squids were qualitatively similar to those of animals in the large culture tanks at the NRCC (pers. obs.). Many of the animals in this study captured and consumed prey (feeder guppies or mysid shrimp) while in the holding tank. None of the squids inked during shipping or during the anesthesia prior to the experiments.

The tether

We measured the thrust produced during escape-jet locomotion in squid tethered to a force transducer. Squid were tethered (see Thompson and Kier, 2001a) as follows. Individual squid were removed from the holding tank and anesthetized lightly in a 1:1 solution of 7.5% $MgCl_2$: artificial seawater (Messenger *et al.,* 1985). A needle (0.3-mm-diameter insect pin for small animals or 0.7-mm-diameter hypodermic needle for large animals) was inserted through the brachial web of the squid, anterior to the brain cartilage and posterior to the buccal mass. The needle was positioned between these two rigid structures to prevent it from tearing the soft tissue of the squid. The needle was inserted into a hollow stainless steel post (hypodermic tubing) attached to a force transducer. Flat, polyethylene washers on the post and needle were positioned above and below the head to prevent vertical movement.

Insertion of the needle through the anesthetized squid was rapid and required minimal handling of the animal. Individuals of *S. lessoniana* become nearly transparent under anesthesia, making the buccal mass and the brain cartilage readily visible. Needle placement was verified after the experiment by examination of the location of the needle entrance and exit wounds.

The tethered squid and force transducer were transferred to an aquarium (0.4 m by 0.2 m by 0.2 m) filled with 20° to 23 °C artificial seawater and were allowed to recover. Recovery, which was judged by the return of normal chromatophore patterning and fin activity, normally occurred within 10 min. Tethered squid remained alive and in apparent good health for up to several hours, though most squid were tethered for fewer than 20 min.

Although tethering is an invasive technique, it did not appear to be unduly traumatic to the squid. First, tethered squid behaved similarly to the animals in the holding tank. Both the tethered and free-swimming squid spent most of the time hovering, using the fins and low-amplitude jets. Second, unlike squid that are in distress or startled, more than 90% of the tethered squid did not eject ink. Third, the chromatophore patterns of tethered squid did not differ qualitatively from the patterns exhibited by freely swimming squid in the holding tank. Finally, when removed from the tether and returned to the holding tank, squid swam normally, and their survival was similar to that of undisturbed specimens. All experiments met the animal care guidelines of the University of North Carolina at Chapel Hill.

Critique of the method

Previously published methods of estimating the thrust produced by jetting squids require measuring the funnel aperture during jet locomotion (see Johnson *et al.,* 1972; O'Dor, 1988a; Anderson and DeMont, 2000). Because a squid can adjust both the orientation of the funnel and the size and shape of the funnel aperture during the jet (Zuev, 1966; O'Dor, 1988a), accurate measurement of funnel diameter is difficult. These problems are exacerbated in newly hatched squid by their inability to maintain position in a flow tank, by their small size, and by the small funnel aperture. In addition, the method employed by Johnson *et al.* (1972) and O'Dor (1988a) is not applicable to hatchling squid because it is not currently possible to monitor mantle cavity pressure in these small animals without substantially altering normal mantle kinematics.

The tethering approach adopted here was chosen to bypass these difficulties. Tethering to a force transducer is particularly effective for small animals (see Svetlichnyy and Svetlichnyy, 1986; Lenz and Hartline, 1999), and the method has the considerable advantage of not requiring the small and dynamic funnel aperture of hatchling and juvenile squids to be measured to calculate thrust. Nevertheless, a potential disadvantage of this approach is its interference with the movement of the mantle during the escape jet. Because the tether did not touch the mantle and the kinematics of the mantle of tethered squids were qualitatively similar to those of untethered squids swimming in the holding tank (see Thompson and Kier, 2001a), it is unlikely that this was a source of significant error. Another possible disadvantage is that the flow field around a tethered squid is stationary. During an escape jet, an untethered squid has a velocity relative to the water, and this velocity affects the magnitude of the thrust required to keep a squid jetting at a given velocity (Vogel, 1994). Because we were investigating the maximum thrust that a squid can generate and not the variations in thrust produced during jetting, the stationary flow field is not an issue. The final potential disadvantage is that the post of the tether, which was located downstream of the funnel aperture (Fig. 1A), could alter thrust by interfering with the fluid exiting the funnel aperture. Significant alterations in thrust caused by the post are considered unlikely because of its small size relative to the funnel aperture and the distance of the post from the funnel aperture. Additionally, there were no significant differences between the thrust measured using either of our force trans-

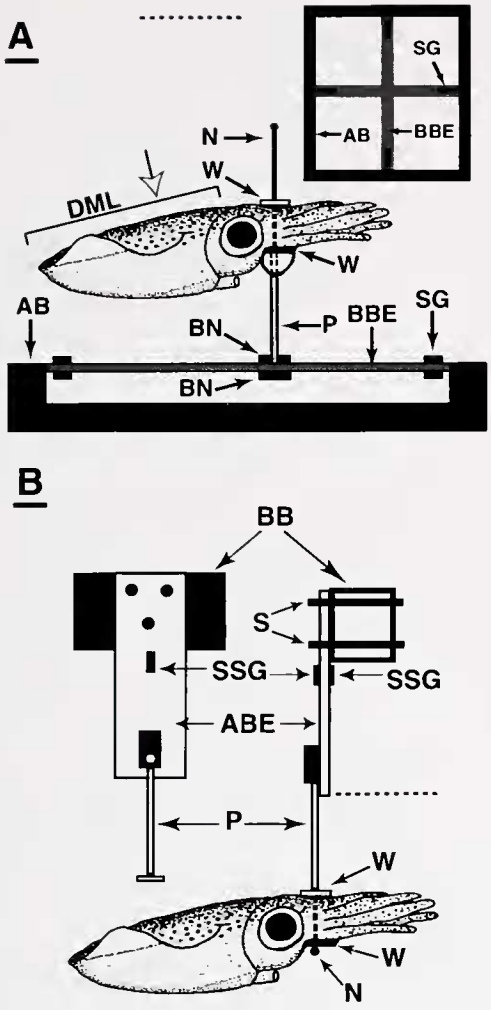

Figure 1. The tethering apparatus and the force transducers. The dashed lines indicate the water level during the experiments. (A) Transducer 1. The inset at top right is a plan view of the schematic with the squid and tether apparatus removed. The bracket above the squid indicates the dorsal mantle length (DML), and the white arrow points to 1/3 DML. AB, aluminum base; BBE, brass blade element; BN, brass nut; N, needle; P, stainless steel post; SG, thin foil strain gauge; W, plastic washer. (B) Transducer 2. The inset at left is a front view of the transducer with the squid removed. Abbreviations same as in A except as follows: ABE, aluminum blade element; BB, box beam; S, screws; SSG, semiconductor strain gauge.

ducers: one which had the post located downstream of the funnel and one which did not (see Fig. 1).

The force transducers

We built two force transducers to measure the thrust produced by the squid. The first force transducer (transducer 1) consisted of thin foil strain gauges, wired as a full bridge (see Biewener and Full, 1992), and glued to two brass blade elements (Fig. 1A; see Appendix for details). We used long, thin blade elements to obtain the sensitivity necessary to measure the small thrust forces of the hatchlings. Thus, the resonant frequency of the force transducer was fairly low (about 55 Hz when unloaded in air).

We also built a second force transducer (transducer 2) with a higher resonant frequency (about 110 Hz when unloaded in air). It consisted of a single aluminum blade element with semiconductor strain gauges wired as a half bridge (Fig. 1B, see Appendix). The higher gauge factor of the semiconductor strain gauges allowed the stiffness of the blade element to be increased without sacrificing sensitivity.

Using analysis of covariance (Glantz and Slinker, 2001), we compared the data from the two force transducers. The adjusted slopes and means of the two data sets did not differ significantly (ANCOVA, $P = 0.82$). Therefore, we pooled the data from both transducers.

Each force transducer was calibrated in air after completion of the day's experiments.

Thrust measurement and mantle kinematics

Escape-jet behavior of squids tethered to the force transducers was videotaped using an S-VHS video camera (Panasonic AG-450 Professional). A light-emitting diode (LED) flashing at 15 Hz was placed in the field of view of the camera to aid in aligning the video fields with the transducer output. The video output, the pre-amplified output voltage from the force transducer, and the 15-Hz signal from the function generator connected to the LED were collected simultaneously on a magnetic tape data recorder (A. R. Vetter Co., Rebersburg, PA).

Escape-jet data were digitized from the magnetic tape at 500 Hz using MacScope MAC-600 (Thornton Associates, Waltham, MA) and DATAQ DI-700 (DATAQ Instruments Inc, Akron, OH) analog-to-digital converters, and analyzed using MacScope and WinDAQ waveform analysis software.

Prior to digitization, the raw thrust-time data from transducer 1 were filtered with a 45-Hz low-pass filter (4 pole Butterworth; Ithaco, Inc., Ithaca, NY). Because (1) the fundamental frequency of the escape jets varied from 5 to 10 Hz, and (2) the contribution to the raw thrust-time data by harmonics above the 4th order was negligible for all the escape jets measured (indeed, the raw thrust-time data of most escape jets were composed of the fundamental and only the first two harmonics), the filtering did not affect the peak forces recorded. The raw data from transducer 2 were not filtered because the signal-to-noise ratio was very high.

Video sequences of escape-jet behavior were viewed using a Panasonic AG-1980P professional S-VHS videocassette recorder. Individual video fields were digitized with a frame grabber card (Imagenation, Beaverton, OR) and changes in mantle diameter measured using morphometrics software (SPSS Science, Chicago, IL). During an escape jet, the outer diameter of the mantle at 1/3 DML (from the

anterior margin of the mantle; see Fig. 1A) was measured in each video field from the S-VHS videotapes and plotted against time. The diameter at 1/3 DML was selected because this location experiences the largest amplitude change during the escape jet (Thompson and Kier, 2001a). Time was estimated from the video camera capture rate of 60 fields per second.

The LED and its voltage spike were used to align the mantle kinematics and thrust data. The plot of thrust *versus* time (*i.e.*, the calibrated output of the force transducer) for the same escape jet was compared with the mantle kinematics.

Data analysis

The peak thrust produced during an escape jet was measured as the difference between the baseline and the highest thrust achieved during the escape jet. The average of the 25 digitized data points (50 ms) immediately preceding the start of the escape jet was used as the baseline. The average of five digitized data points (10 ms) at the highest thrust produced was considered the peak thrust. The peak thrust was measured in a minimum of eight escape jets for each squid and only the largest thrust reported.

We also determined the average rate of thrust increase during each escape jet. This rate was calculated as the average slope of the thrust-time trace over the interval from the start of the jet to the peak thrust. Only the highest average rate for each squid was reported. In most instances, the escape jet that yielded the highest peak thrust also had the highest average slope.

We calculated impulse over the interval from the start of the escape jet to the point at which the thrust-time trace returned to the baseline (see arrows in Fig. 2B). Impulse is the integral of the product of force and time, and is a measure of the change in momentum of a squid during an escape jet. The impulse was calculated for a minimum of eight escape jets for each squid, and only the largest impulse was reported.

Morphometrics of mantle and funnel

We normalized the thrust data for each squid in two ways. First, we divided the peak thrust of the escape jet by the wet weight of the squid to yield the weight-specific thrust. To determine weight, squids were anesthetized, lifted from the anesthetic by the posterior tip of the mantle (to permit water to drain from the mantle cavity), blotted dry, and weighed to the nearest 5 mg on an electronic balance.

Second, we divided the peak thrust by the cross-sectional area of the mitochondria-poor circumferential muscles of the mantle. These muscles, analogous to the white muscle fibers of mammals (Bone *et al.*, 1981; Mommsen *et al.*, 1981), are a relevant measure because it is likely that they provide the power for escape-jet locomotion (Gosline *et al.*, 1983; Bartol, 2001). Cross-sectional area of the "white" circumferential muscles was estimated as follows. The thickness of the ventral midline of the mantle at 1/2 DML was measured in unfixed squids. The squids were anesthetized in 7.5% $MgCl_2$ and killed by decapitation. Blocks of tissue from the midline of the ventral mantle were then fixed and embedded in paraffin. Sections parallel to the sagittal plane (*i.e.*, transverse to the long axes of the circumferential muscle fibers) were cut at 5 μm and stained. The ratio of the thickness of the band of white circumferential muscle fibers to the thickness of the entire mantle wall was measured from stained sections. Using the initial measurement of mantle thickness in unfixed animals, the width of the white circumferential muscle band could then be determined. The cross-sectional area of the muscles was estimated by multiplying the DML by the width of the white muscle band.

We also measured the maximum funnel aperture in a subset of the sample population. The diameter was measured with an ocular micrometer in squids that had been anesthetized following tethering.

Statistics

The sample population used in this study was subdivided into the life-history stages described by Segawa (1987). The life-history stages were selected as an independent organization scheme upon which to base many of the statistical analyses. Segawa (1987) studied the life cycle of *S. lessoniana* from embryo to adult and divided the life cycle into seven stages based on morphological and ecological characters. These stages include hatchling (up to 10 mm DML), juvenile 1 (11–25 mm DML), juvenile 2 (26–40 mm DML), young 1 (41–60 mm DML), young 2 (61–100 mm DML), subadult (100–150 mm DML), and adult (>150 mm DML). In this classification, external adult morphology is achieved around 40 mm DML (the end of the juvenile 2 stage), and onset of sexual maturity occurs at 150 mm DML. The sample population of *S. lessoniana* used in the current investigation included the hatchling, juvenile 1, and juvenile 2 stages.

Nonparametric statistics were used for most of the analyses. For comparisons among the life-history stages, Kruskal-Wallis one-way analysis of variance on ranks was used with Dunn's method of pairwise multiple comparisons (Zar, 1996). Comparisons among all squid in the ontogenetic series were made using the Spearman rank order correlation (Zar, 1996).

All log-transformed (base 10) data passed normality and homoscedasticity tests. Regression lines were fitted to the data using an ordinary least squares approximation. All statistical analyses were completed using SigmaStat 1.01 (SPSS Science, Chicago, IL) and JMP (SAS, Cary, NC).

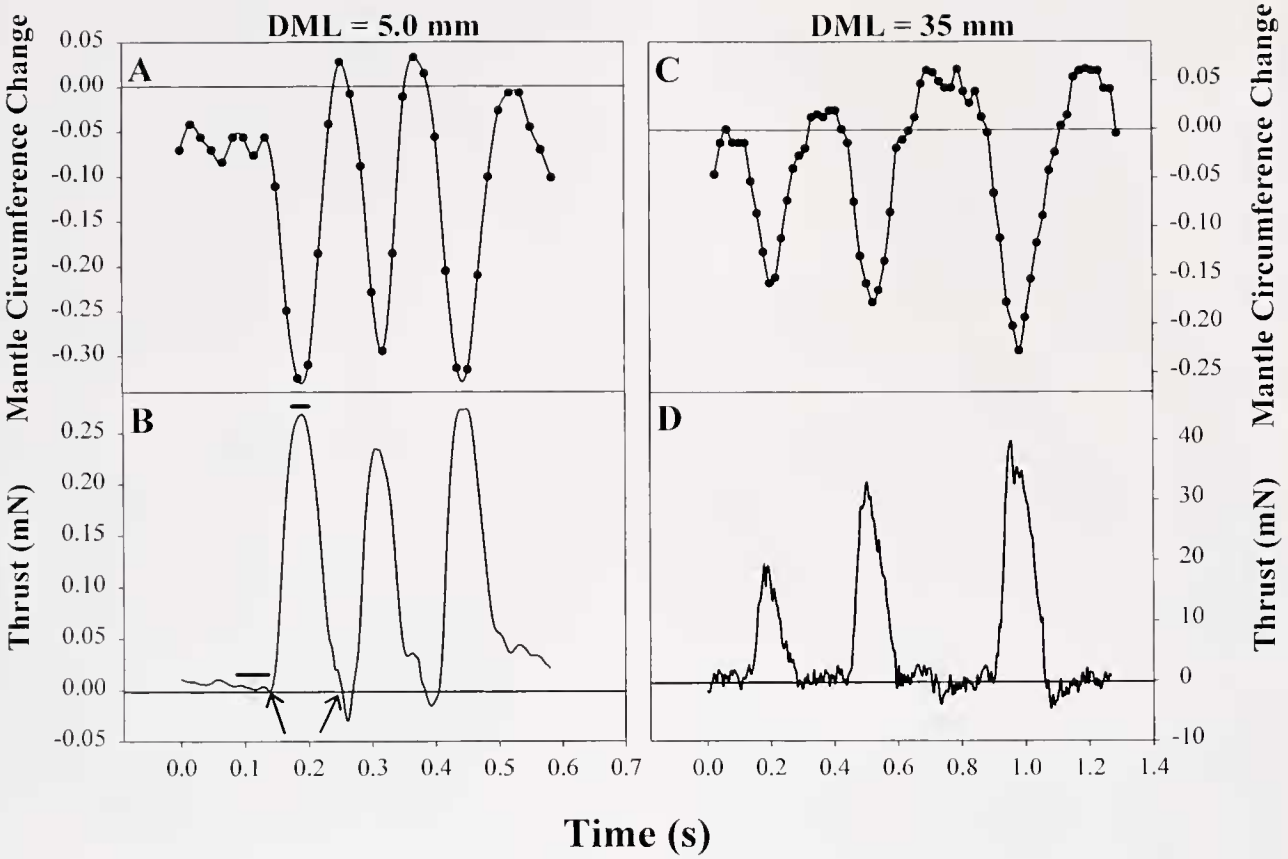

Figure 2. Plot of mantle circumference change and thrust *versus* time during three escape jets in a hatchling (DML, 5 mm) and a juvenile 2 (DML, 35 mm) stage of the squid *Sepioteuthis lessoniana*. (A and C) Mantle circumference change was normalized by the resting mantle diameter at 1/3 DML (represented by the horizontal lines) in the anesthetized squid. Negative values indicate contraction of the mantle; positive values indicate hyperinflation. Each data point represents the mantle circumference measurement from a single video field. (B and D) Plots of thrust *versus* time for the same sequences of escape-jetting in panels A and C, respectively. The trace in panel B was from transducer 1. The raw data were filtered at 45 Hz (low pass). The arrows on the plot indicate the interval over which the impulse was calculated. The black bar to the left of the first escape jet indicates the 50-ms interval used to calculate the average baseline thrust. The small bar at the top of the first escape jet indicates the 10-ms interval used to calculate the peak thrust. The trace in panel D is from transducer 2. The raw data are presented.

Results

Thrust-time traces

There were no major qualitative differences in the shape of the thrust-time traces during ontogeny. At the start of an escape jet the mantle usually expands beyond its resting diameter. During this "hyperinflation," water fills the mantle cavity through large openings along the left and right anterior edges of the mantle. The plots of thrust *versus* time often showed negative thrust that was correlated with hyperinflation of the mantle as observed in the video records (Fig. 2).

Next in the escape-jet sequence, the mantle contracts rapidly and ejects water from the mantle cavity through the funnel aperture. Concurrent with contraction of the mantle, thrust increased rapidly (Figs. 2B, D). In hatchling stage squid, the thrust peaked within 40 ms ± 7.4 ms (mean ± standard deviation) of the start of the escape-jet, whereas in juvenile 2 stage squid thrust peaked within 71 ms ± 14 ms.

In the final event of the escape-jet sequence, the mantle re-expands to its original shape and the mantle cavity is refilled. At the end of the mantle contraction and during mantle refilling, the thrust decreased rapidly, though at a lower rate than the force increase during the early phase of mantle contraction (Fig. 2B, D). In many of the thrust-time traces, though most noticeably in the juvenile 1 and juvenile 2 stage animals, the thrust decreased below the baseline during refilling of the mantle cavity, implying reverse thrust (the end of jet 1 in Fig. 2B; at the end of jet 3 in Fig. 2D).

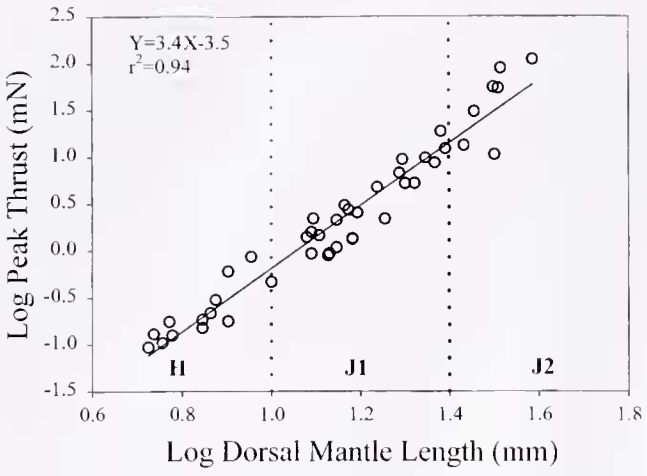

Figure 3. The log of the peak thrust generated during the escape jet *versus* the log of dorsal mantle length. Each data point represents the highest peak thrust produced by one squid, and thus there are no error bars. Log peak thrust was regressed against the log of the DML, using an ordinary least-squares method. The equation is indicated in the upper left corner of the plot. H, Hatchling stage squids; J1, Juvenile 1 stage; J2, Juvenile 2 stage.

Peak thrust

As expected, the peak thrust produced during the escape jet increased with dorsal mantle length (Spearman rank order correlation, $r = 0.97$, $P < 0.001$, $n = 54$). Newly hatched *S. lessoniana* produced between 0.10 mN and 0.80 mN of thrust during the eseape jet, whereas the largest squids studied generated between 18 mN and 110 mN of thrust (Fig. 3; see Table 1 for descriptive statistics based on life-history stage). Sorting the data by the life-history stages of Segawa (1987) indicated that hatchling stage squid generated lower peak thrust than either the juvenile 1 or juvenile 2 stage squid ($P < 0.01$; Table 1). Juvenile 1 stage squid produced lower peak thrust than juvenile 2 stage animals during the escape jet ($P < 0.01$; Table 1).

The peak thrust data were normalized by the wet weight of each squid. The weight-specific peak thrust of the escape jet increased significantly with DML (Spearman rank order correlation, $r = 0.68$, $P < 0.001$, $n = 54$), from 0.20 to 0.40 in hatchlings to between 1.0 and 2.5 in the largest squids tested (Fig. 4A). Sorting the data by the life-history stages of Segawa (1987) indicated that the mean of 0.36 in the hatchling stage squid was significantly lower than the averages of 0.55 and 1.5 in the juvenile 1 and juvenile 2 stage squids, respectively ($P < 0.01$; Table 1). In addition, the juvenile 1 stage animals produced lower weight-specific thrust during the escape-jet than did the juvenile 2 stage squids ($P < 0.01$; Table 1).

The peak thrust data were also normalized by the cross-sectional area of the "white" circumferential muscle fibers (*i.e.*, the muscles that probably provide the power for escape-jet thrust; see Gosline *et al.*, 1983, and Bartol, 2001). Newly hatched squids generated much lower thrust per unit area of white circumferential muscle than did older, larger animals (Fig. 4B). Sorting the normalized thrust data by the life-history stages of Segawa (1987) indicated that hatchling stage squids produced significantly lower thrust per unit area of white circumferential muscle (0.25 mN/mm^2) than either the juvenile 1 (0.47 mN/mm^2) or juvenile 2 (1.4 mN/mm^2) stage squids ($P < 0.01$; Table 1). In addition, the juvenile 1 stage squids produced lower normalized thrust than juvenile 2 stage animals ($P < 0.01$; Table 1).

Rate of thrust increase

The average rate of thrust increase of the escape jet increased significantly with dorsal mantle length (Spearman rank order correlation, $r = 0.92$, $P < 0.001$, $n = 54$). The mean rate of thrust increase varied from 3 to 18 mN/s in hatchlings and increased rapidly to between 300 and 1800 mN/s in the largest squids studied (Fig. 5). Sorting the data by the life-history stages of Segawa (1987) indicated that the average rate of thrust increase in hatchling stage animals (13 mN/s) was significantly lower than in either the juvenile

Table 1

A comparison of the mechanics of the escape jet among squid divided into the life-history stages of Segawa (1987)

Stage	*n*	Peak thrust (mN)	Weight-specific peak thrust	Thrust/unit area muscle (mN/mm^2)	Mean rate thrust increase (mN/s)	Mean impulse (mN · s)
Hatchling	17	0.28 ± 0.24	0.36 ± 0.15	0.25 ± 0.10	13 ± 13	1.3 ± 1.2
Juvenile 1	27	4.0 ± 3.2	0.55 ± 0.24	0.47 ± 0.18	170 ± 240	30 ± 32
Juvenile 2	10	45 ± 32	1.5 ± 0.78	1.4 ± 0.72	960 ± 190	600 ± 370

The means of the peak thrust, the weight-specific peak thrust, the thrust per unit area of "white" circumferential muscle, the rate of thrust increase, and impulse during the escape jet are listed in each column ± the standard deviation of the mean. The highest thrust, weight-specific thrust, thrust/unit area muscle, rate of thrust increase, and impulse for each squid in a life-history stage were pooled to calculate the mean and the standard deviation. In each column, the mean value for the hatchling stage squids was significantly less than the mean for the juvenile 1 and juvenile 2 life-history stages (one-way ANOVA on ranks, $P < 0.01$). In each column, the mean value for the juvenile 1 stage squids was significantly less than the mean for the juvenile 2 stage animals (one-way ANOVA on ranks, $P < 0.01$).

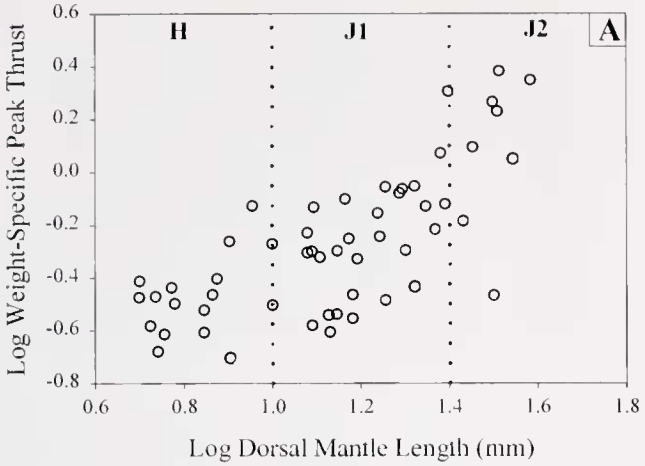

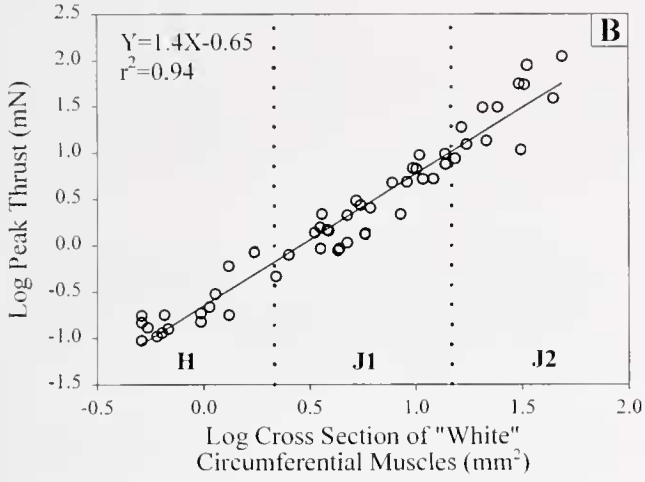

Figure 4. The peak thrust of the escape jet normalized by different measures of squid size. H, Hatchling stage squids; J1, Juvenile 1 stage; J2, Juvenile 2 stage. (A) The log of weight-specific peak thrust produced during the escape jet *versus* the log of dorsal mantle length. Weight-specific peak thrust was calculated by dividing the peak thrust generated by an individual squid (data in Fig. 3) by the wet weight (in mN) of the squid. Weight-specific peak thrust was positively correlated with DML (Spearman rank order correlation, $r = 0.68$, $P < 0.001$, $n = 54$). (B) The log of the peak thrust of the escape jet *versus* the log of the cross-sectional area of the "white" circumferential muscles. Log peak thrust was regressed against the log of the cross-sectional area of the white circumferential muscles, using an ordinary least-squares method. The equation is indicated in the upper left corner of the plot.

1 (170 mN/s) or juvenile 2 (960 mN/s) stages ($P < 0.01$; Table 1). The rate of thrust increase was also lower in juvenile 1 stage animals than in juvenile 2 stage squids ($P < 0.01$; Table 1).

Impulse

The impulse produced during the escape jet increased rapidly with DML (Spearman rank order correlation, $r = 0.88$, $P < 0.001$, $n = 54$). Impulse ranged from 0.25 to 5.0 mN · s in newly hatched animals and increased expo-

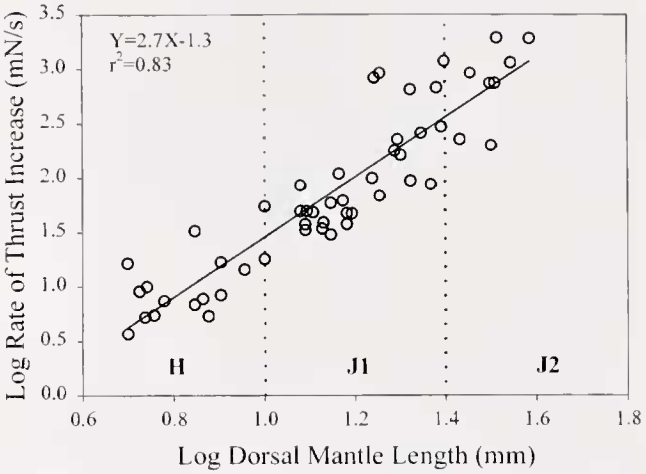

Figure 5. Plot of the log rate of thrust increase *versus* the log of dorsal mantle length. Each point represents the highest rate of thrust increase for one squid. Log rate of thrust increase was regressed against the log of DML, using an ordinary least-squares method. The regression equation is located in the upper left corner of the plot. H, Hatchling stage squids; J1, Juvenile 1 stage; J2, Juvenile 2 stage.

nentially during ontogeny to between 100 and 1000 mN · s in the largest squids studied (Fig. 6). Sorting the data into the life-history stages of Segawa (1987) indicated that the mean impulse of 1.3 mN · s in the hatchling stage squid was significantly less than the impulses of 30 mN · s and 600 mN · s in the juvenile 1 and 2 stage animals, respectively ($P < 0.01$; Table 1). In addition, the juvenile 1 stage squid

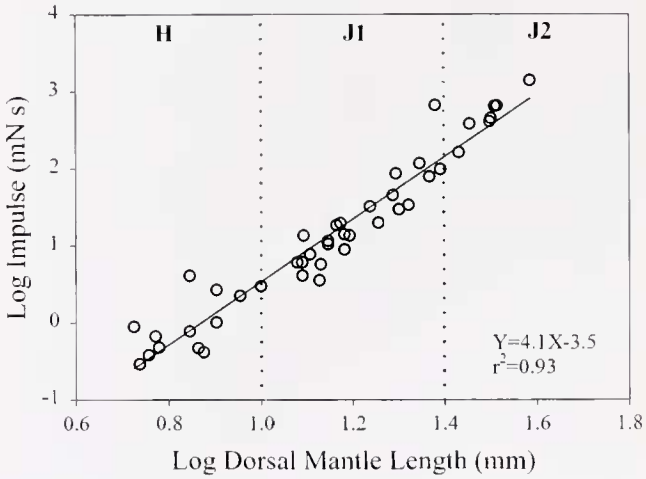

Figure 6. Plot of log impulse *versus* log dorsal mantle length. Each point represents the highest impulse produced during an escape jet by one squid. The impulse (the integral of force · time) was calculated from the force and time data for each escape jet. In most cases, the highest impulse was produced during the same escape jet that yielded the peak thrust. Log impulse was regressed against the log of DML, using an ordinary least-squares method. The regression equation is located in the lower right corner of the plot. H, Hatchling stage squids; J1, Juvenile 1 stage; J2, Juvenile 2 stage.

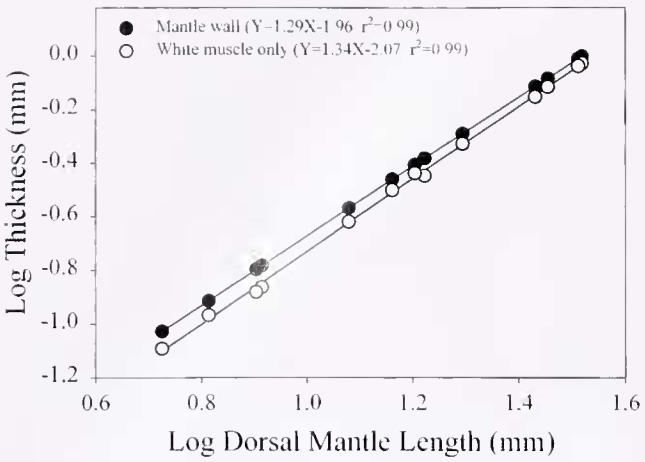

Figure 7. Mantle morphometric data. Log thickness of the mantle wall (filled symbols) and log thickness of the layer of "white" circumferential mantle muscles (open symbols) *versus* log dorsal mantle length. The thickness of both the entire mantle wall and the layer of white circumferential muscles was measured at ½ dorsal mantle length along the ventral midline. See the materials and methods section for details. Log mantle thickness and log thickness of the white muscles were regressed against the log DML, using an ordinary least-squares method. The regression equations are located in the upper left corner of the plot. Note the positive allometry: relative to mantle length, both the thickness of the mantle wall and the layer of white muscles are highest in the oldest, largest animals studied.

produced less impulse during the escape jet than the juvenile 2 stage animals ($P < 0.01$; Table 1).

Morphometrics of mantle and funnel

The thickness of the mantle wall increased from between 0.070 mm and 0.13 mm in hatchlings, up to 2.5 mm in the largest animals studied (Fig. 7). The slope (1.29) of the regression of the thickness of the mantle wall against DML and the slope (1.34) of the regression of the thickness of the white circumferential muscle layer against DML were significantly greater than 1.0 ($P < 0.01$). This indicates positive allometry of mantle thickness, relative to DML, during growth (Fig. 7). In addition, the slopes of the two regressions were not significantly different ($P > 0.05$), suggesting that the positive allometric increase in mantle wall thickness (relative to DML) was due, in large part, to the ontogenetic allometric increase in the width of the white circumferential muscle layer (Fig. 7).

The diameter of the funnel aperture in anesthetized squids increased during growth. The slope (0.65) of the regression of funnel aperture against DML was, however, less than unity, indicating that the aperture of the funnel relative to body length decreased with growth (Fig. 8). Indeed, the average funnel aperture in anesthetized newly hatched squids is about 1.8 times larger (relative to mantle length) than the average aperture in anesthetized juvenile 2 stage squids.

Discussion

The peak thrust, weight-specific peak thrust, rate of thrust increase, and impulse of the escape jet all increase significantly during the growth of *S. lessoniana*. These changes in the mechanics of the escape jet correlate strongly with striking ontogenetic changes in (1) the morphology of the mantle (Thompson and Kier, 2001b) and funnel, and (2) the maximum amplitude and rate of mantle movement during the jet (Thompson and Kier, 2001a). Furthermore, the changes in the mechanics of the escape jet have implications for circumferential muscle mechanics and the propulsion efficiency of the jet.

Ontogeny of muscle mechanics

The large increase in the relative thickness of the musculature of the mantle wall (Fig. 7) may help explain the ontogenetic increase in the weight-specific thrust of the escape jet (Fig. 4A). For a pressurized cylinder such as the mantle, the relationship between the stress in the wall, the pressure, and the radius is given by the following equation (after Fung, 1994):

$$\sigma = r_i p/t \qquad \text{(Eq. 2)}$$

where σ is the average circumferential stress in the wall, p is the internal pressure, r_i is the radius of the inner edge of the mantle wall, and t is the thickness of the mantle wall. Solving equation (2) for pressure (p),

$$p = \sigma t/r_i \qquad \text{(Eq. 3)}$$

and substituting measured values of mantle radius (Thompson

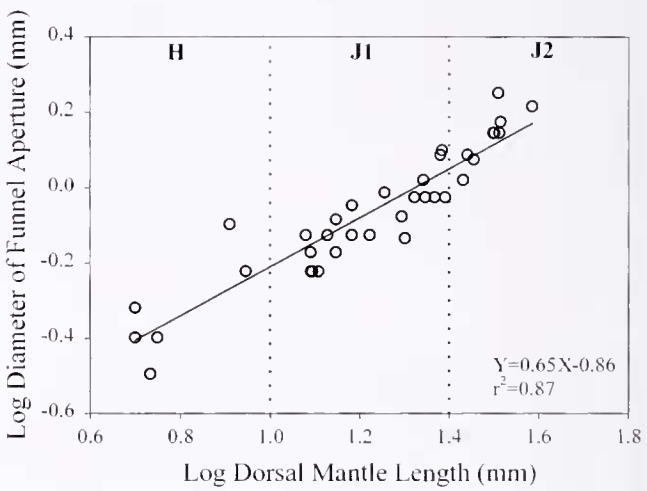

Figure 8. Log diameter of the funnel aperture *versus* log dorsal mantle length. Maximum funnel aperture was measured in anesthetized squids. The regression was done using an ordinary least squares method, and the equation is listed in the lower right corner of the plot. Note the negative allometry of the relationship: the funnel aperture is largest (relative to mantle length) in the smallest squids. H, Hatchling stage squids; J1, Juvenile 1 stage; J2, Juvenile 2 stage.

and Kier, 2001a), of mantle wall thickness (Fig. 7A), and of the peak isometric stress generated by the circumferential mantle muscles of squids (Milligan *et al.*, 1997), the maximum mantle cavity pressure that can be generated during the escape jet can be calculated. The peak isometric stress produced by the "white" circumferential mantle muscles of adult *Loligo vulgaris* was measured to be 262 mN/mm^2, but it may range as high as 400 mN/mm^2 (Milligan *et al.*, 1997). Using those values and assuming that the peak isometric stress of the circumferential muscles does not change during ontogeny, we calculate that a newly hatched squid (DML = 5 mm) should generate mantle cavity pressures between 2 and 3 kPa during the escape jet, whereas a juvenile squid (DML = 40 mm) should produce pressures between 6 and 9 kPa. This threefold difference in the maximum mantle cavity pressure during the escape jet results from a substantial ontogenetic increase in the relative thickness of the mantle wall musculature and may explain part of the ontogenetic increase in the weight-specific peak thrust of the escape jet that we observed.

The ontogenetic difference in the relative thickness of the mantle wall alone is insufficient to explain the growth-related changes in the mechanics of the escape jet. Our data also suggest that the contractile properties of the circumferential mantle muscles of *S. lessoniana* change during growth. Newly hatched squid generated 0.25 mN thrust per square millimeter of circumferential muscle during the escape jet, whereas the largest squids studied were able to produce nearly 6 times as much thrust per unit area of muscle (Fig. 4B; Table 1). Although the mantles of hatchlings contain a slightly lower proportion of the white circumferential muscle fibers that provide the power for the escape jet than the mantles of adults (Thompson and Kier, 2001b), ontogenetic differences in the proportions of "red" and "white" circumferential muscle fibers are insufficient to explain the sixfold difference in thrust per unit area that we observed. Indeed, normalizing the peak thrust data by the entire thickness of the mantle wall (*i.e.*, both the red and white circumferential muscles) does not change the result.

The thrust produced per unit area of circumferential muscle depends not only on the contractile properties of the circumferential muscles (*e.g.*, thick myofilament length), but also on the funnel aperture. Control of the funnel aperture affects the peak thrust of the escape jet and, therefore, the measurement of the "unit thrust output" of the circumferential musculature. Thus, the ontogenetic differences in the magnitude of thrust per unit area of the circumferential muscles may depend on several variables.

An additional observation, however, supports the proposal that the contractile properties of the mantle muscle change with growth. Thompson and Kier (2001a) reported that the shortening velocity of the circumferential muscles (measured indirectly from the contraction velocity of the entire mantle during an escape jet) ranged from a high of 13 lengths per second (L/s) in hatchling *S. lessoniana* to a low of 4 L/s in mature squids. The shortening velocity of muscle varies inversely with the load on the muscle and the lengths of the thick filaments and sarcomeres, and in direct proportion to the rate of cross-bridge cycling (Schmidt-Nielsen, 1997). The force generated by a muscle varies in proportion with its cross-sectional area and the length of its thick filaments (Schmidt-Nielsen, 1997). Thus, shorter thick filaments in hatchling *S. lessoniana* than in older, larger squids would be consistent with the observations that (1) the shortening velocity of the circumferential muscles is highest in hatchlings, and (2) the peak thrust generated per unit area circumferential muscle is lowest in hatchlings. We plan to measure the contractile properties and myofilament dimensions of the circumferential muscles from an ontogenetic series of *S. lessoniana* to examine the possibility of a change in performance of the muscle during ontogeny.

Propulsion efficiency

The propulsion efficiency of jet locomotion may be higher in newly hatched individuals of *S. lessoniana* than in older, larger animals. Propulsion efficiency is the ratio of the power output by the animal (the product of thrust and the velocity of the animal) to the power input by the animal (the kinetic energy input per unit time). The hydrodynamic propulsion efficiency (η) of the exhalant phase of the jet stroke can be calculated using the following equation of rocket-motor propulsion efficiency:

$$\eta = (2VV_j)/(V^2 + V_j^2), \text{(Anderson and DeMont, 2000)} \quad \text{(Eq.4)}$$

where V is the velocity of flow past the squid and V_j is the velocity of the jet relative to the squid. According to equation (4), the highest propulsion efficiency is achieved when V_j approximates V. Because V_j must be greater than V for a squid to accelerate, a relatively lower jet velocity increases propulsion efficiency.

Our results support the hypothesis that V_j is relatively lower in hatchling than in larger *S. lessoniana* individuals. First, the funnel is proportionately larger (about 1.8 times, relative to body size) in anesthetized newly hatched squids than in older, larger squids (Fig. 8; also see Clarke, 1966; Packard, 1969; Boletzky, 1974). By the principle of continuity, for a given volume of water exiting the mantle cavity per unit time, a larger funnel aperture will decrease the average water velocity, while a narrow nozzle will increase the average water velocity.

Second, steady-state jet thrust is proportional to the product of mass flux (= mass of water per unit time that exits the mantle cavity) and the difference between the velocity of water exiting the funnel aperture and the velocity of the animal (Vogel, 1994). In previous work on *S. lessoniana* (Thompson and Kier, 2001a), we showed that significant differences in the relative volume of water in the mantle

cavity and both the amplitude and the rate of mantle contraction during escape-jet locomotion result in much greater relative mass flux in hatchlings than in larger squid. Because the peak weight-specific thrust produced during the escape jet is lowest in newly hatched squid (Fig. 4A, Table 1) but relative mass flux is highest (Thompson and Kier, 2001a), the velocity of water exiting the funnel aperture (V_j) must be relatively slower in the hatchlings than in the adults. This observation supports the assumption that the funnel apertures of hatchling squids are relatively larger than the apertures of mature squids, not only in anesthetized animals but also during escape-jet locomotion (see also O'Dor and Hoar, 2000).

Is the propulsion efficiency of the escape jet higher in newly hatched squid than in larger animals? Anderson and DeMont (2000) emphasize that the overall propulsion efficiency of the jet includes both the efficiency of the jet stroke and the efficiency of refilling the mantle cavity. The thrust-time traces for the escape jets of many squid showed that a substantial thrust, opposite in direction to the escape-jet thrust, occurs during the refilling of the mantle cavity. We suspect that these forces are associated with refilling following the escape jet. However, further work with higher time resolution video data is required to begin to measure the efficiency of refilling.

If the propulsion efficiency of the exhalant phase of the escape jet is higher in newly hatched squid than in larger animals, is the cost of transport during escape-jet locomotion lower in hatchlings? Most likely, it is not. Mass-specific metabolic rate is higher in hatchling ommastrephid and loliginid squids than in the adults (O'Dor and Webber, 1986; O'Dor, 1988b). In addition, hydromechanical costs other than propulsion efficiency, such as drag and the acceleration reaction, may be relatively higher in the intermediate Reynolds number (Re) fluid regime of the hatchling squid. For example, Müller *et al.* (2000) hypothesized that burst-and-coast swimming was much less efficient hydrodynamically in larval zebra danios (*Brachydanio rerio*) than in the adult fish. Because the larval fish swim in an intermediate Re fluid regime, Müller *et al.* (2000) suggested that the high relative viscous drag on the larvae during the coasting phase contributed to the reduction in hydrodynamic efficiency relative to the adult. Indeed, *B. rerio* larvae coast for less than half a body length, but adult fish coast for several body lengths following a burst (Müller *et al.*, 2000).

Escape-jet locomotion is analogous to burst-and-coast swimming. In escape-jet locomotion, there is a brief period of thrust generation (*i.e.*, rapid contraction of the mantle) followed by mantle cavity refilling and coasting. Given their small size and low absolute swimming speeds, newly hatched squids swim in an intermediate Re fluid regime (unpub. obs. of *S. lessoniana*; Hoar *et al.*, 1994; Preuss *et al.*, 1997). Because viscous drag is relatively high at intermediate Re, newly hatched individuals of *S. lessoniana* may experience lower hydrodynamic efficiency relative to the adult during escape-jet locomotion. Unfortunately, it is not possible to analyze this issue further because, to our knowledge, there are no data on the hydrodynamics of escape-jet locomotion in hatchling squid. Nevertheless, higher propulsion efficiency for hatchlings of *S. lessoniana* will reduce the cost of transport, compared to a hypothetical case in which the kinematics and mechanics of the escape jet in hatchlings are identical to those of the adults.

Finally, the relatively large funnel apertures of hatchlings of *S. lessoniana* will result in lower velocities of water exiting the funnel (V_j) at all jetting speeds, not only in escape-jet locomotion. Indeed, it is likely that natural selection for high propulsion efficiency during the escape jet is not strong in hatchlings (*i.e.*, the cost of being eaten is zero fitness). Thus, the relatively large funnel apertures in hatchlings may represent selection for high propulsion efficiency at low-speed jetting, with the associated trade-off of low weight-specific thrust of the escape jet. An alternative hypothesis is that size-related differences in the physics of locomotion may constrain funnel aperture in the tiny hatchlings.

An effect of scale on jet locomotion?

In *S. lessoniana*, ontogenetic changes in the mantle kinematics of the escape jet occur concomitantly with a reorganization of the intramuscular (IM) collagen fibers that store elastic energy and help limit the deformation of the mantle during jet locomotion (Thompson and Kier, 2001b). One consequence of these changes in mantle morphology and function is that the average mass flux of the escape jet, relative to body mass, is highest in hatchling squids and declines significantly during growth (Thompson and Kier, 2001a). As mentioned previously, jet thrust is proportional to the product of mass flux and the velocity of water exiting the funnel aperture (Vogel, 1994). Because the weight-specific peak thrust of the escape jet is lowest in hatchlings, the velocity of water exiting the funnel must be disproportionately low in newly hatched animals. Thus, tiny squid must keep the funnel aperture relatively large during the escape jet.

If mass flux remains unchanged, hatchlings could increase the weight-specific peak thrust generated during the escape jet by narrowing the funnel aperture. Given the potential benefits of increasing the weight-specific thrust, why don't hatchlings narrow the funnel aperture during the escape jet? One possibility is that newly hatched squid are unable to modulate the aperture of the funnel, perhaps due to mechanical or neuromuscular limitations of the funnel musculature. However, because the pressure required to pump water through a pipe (*e.g.*, a funnel) at a given rate of flow varies inversely with the 4th power of the radius of the pipe (Vogel, 1994), two alternative hypotheses are also

possible. First, the circumferential muscles (that create the pressure that forces water through the funnel) of hatchlings might not produce sufficient force to maintain relatively high mass flux through a smaller funnel aperture. Second, the circumferential muscles of hatchlings might be able to generate sufficient force, but the energetic costs of forcing water through a relatively smaller funnel may be higher. Thus, an effect of scale may have constrained the evolution of funnel aperture in *S. lessoniana*. We are attempting to address this issue by measuring the mechanics of the circumferential muscles in an ontogenetic series of *S. lessoniana* and by using a comparative approach to study the prevalence of ontogenetic changes in the organization of IM collagen fibers in the mantles of a variety of cephalopods.

Summary and future directions

In conclusion, we observed significant ontogenetic changes in the mechanics of the escape jet in squid tethered to a force transducer. These growth-related alterations in the mechanics of the escape-jet may be correlated with changes in the mechanics of the circumferential muscles of the mantle. The changes reveal an apparent trade-off in jet locomotion during growth—hatchling squids achieve high propulsion efficiency, but at the expense of the thrust. This apparent trade-off may be indicative of an effect of scale on jet locomotion.

As the next step, we intend to measure the ontogeny of locomotor performance (peak escape velocity, acceleration, *etc.*) in untethered specimens of *S. lessoniana*. We also plan to measure the contractile properties and myofilament dimensions of the circumferential muscles from an ontogenetic series of *S. lessoniana* in order to examine the possibility of a change in performance of the muscle during ontogeny. In addition, because the elastic energy stored during mantle hyperinflation may be returned to augment the thrust produced during the escape jet, future studies should examine the ontogeny of radial muscle contraction in hyperinflation. These experiments will help us achieve our ultimate goal of understanding the fitness consequences of ontogenetic variation in morphology, physiology, and locomotion in soft-bodied invertebrates.

Acknowledgments

This research was supported by NSF grants to W.M.K. (IBN-9728707 and IBN-9219495). Grants and fellowships to J.T.T. from the Wilson Fund, the American Malacological Society, and Sigma Xi helped defray research expenses. The research was also supported by a Seeding Postdoctoral Innovators in Research and Education (SPIRE) fellowship to J.T.T. from the Minority Opportunities in Research Division of the National Institute of General Medical Sciences (Grant No. GM000678). H. Hsiao, R. Goldberg, and S. Vogel provided ideas for the force transducers, and J. Goldman supplied the circuit diagram for the instrumentation amplifier that we built to amplify the thrust-time signals. We thank L. Walsh at the NRCC for her expertise in shipping squid cross-country. We thank J. Taylor, T. Uyeno, J. Voight, and two anonymous reviewers for excellent comments and suggestions.

Literature Cited

Anderson, E. J., and M. E. DeMont. 2000. The mechanics of locomotion in the squid *Loligo pealei*: locomotory function and unsteady hydrodynamics of the jet and intramantle pressure. *J. Exp. Biol.* **203:** 2851–2863.

Bartol, I. K. 2001. Role of aerobic and anaerobic circular mantle muscle fibers in swimming squid: electromyography. *Biol. Bull.* **200:** 59–66.

Batty, R. S. 1984. Development of swimming movements and musculature of larval herring (*Clupea harengus*). *J. Exp. Biol.* **110:** 217–229.

Biewener, A. A., and R. J. Full. 1992. Force platform and kinematic analysis. Pp. 45–73 in *Biomechanics: Structures and Systems. A Practical Approach*, A. A. Biewener, ed. IRL Press at Oxford University Press, New York.

Boletzky, S. V. 1974. The "larvae" of Cephalopoda: a review. *Thalassia Jugosl.* **10:** 45–76.

Bone, Q., A. Pulsford, and A. D. Chubb. 1981. Squid mantle muscle. *J. Mar. Biol. Assoc. UK* **61:** 327–342.

Clarke, M. R. 1966. A review of the systematics and ecology of oceanic squids. *Adv. Mar. Biol.* **4:** 91–300.

Daniel, T., C. Jordan, and D. Grunbaum. 1992. Hydromechanics of swimming. Pp. 17–49 in *Advances in Comparative and Environmental Physiology. Vol. II. Mechanics of Animal Locomotion*, R. M. Alexander, ed. Springer-Verlag, New York.

Fung, Y. C. 1994. *A First Course in Continuum Mechanics: For Physical and Biological Scientists and Engineers.* 3rd ed. Prentice Hall, Englewood Cliffs, NJ.

Gilly, W. F., B. Hopkins, and G. O. Mackie. 1991. Development of giant motor axons and neural control of escape responses in squid embryos and hatchlings. *Biol. Bull.* **180:** 209–220.

Glantz, S. A., and B. K. Slinker. 2001. *Primer of Applied Regression and Analysis of Variance.* 2nd ed. McGraw-Hill, New York.

Gosline, J. M., J. D. Steeves, A. D. Harman, and M. E. DeMont. 1983. Patterns of circular and radial mantle muscle activity in respiration and jetting of the squid *Loligo opalescens*. *J. Exp. Biol.* **104:** 97–109.

Hoar, J. A., E. Sim, D. M. Webber, and R. K. O'Dor. 1994. The role of fins in the competition between squid and fish. Pp. 27–43 in *Mechanics and Physiology of Animal Swimming*, L. Maddock, Q. Bone, and J. M. V. Rayner, eds. Cambridge University Press, Cambridge.

Johnson, W., P. D. Soden, and E. R. Trueman. 1972. A study in jet propulsion: an analysis of the motion of the squid, *Loligo vulgaris*. *J. Exp. Biol.* **56:** 155–165.

Lee, P. G., P. E. Turk, W. T. Yang, and R. T. Hanlon. 1994. Biological characteristics and biomedical applications of the squid *Sepioteuthis lessoniana* cultured through multiple generations. *Biol. Bull.* **186:** 328–341.

Lenz, P. H., and D. K. Hartline. 1999. Reaction times and force production during escape behavior of a calanoid copepod, *Undinula vulgaris*. *Mar. Biol.* **133:** 249–258.

Lighthill, J. 1975. *Mathematical Biofluiddynamics.* Society for Industrial and Applied Mathematics, Philadelphia.

Messenger, J. B., M. Nixon, and K. P. Ryan. 1985. Magnesium chloride as an anaesthetic for cephalopods. *Comp. Biochem. Physiol.* **82C:** 203–205.

Milligan, B. J., N. A. Curtin, and Q. Bone. 1997. Contractile properties

of obliquely striated muscle from the mantle of squid (*Alloteuthis subulata*) and cuttlefish (*Sepia officinalis*). *J. Exp. Biol.* **200:** 2425–2436.

Mommsen, T. P., J. Ballantyne, D. MacDonald, J. Gosline, and P. W. Hochachka. 1981. Analogues of red and white muscle in squid mantle. *Proc. Natl. Acad. Sci. USA* **78:** 3274–3278.

Müller, U. K., and J. J. Videler. 1996. Inertia as a 'safe harbour': Do fish larvae increase length growth to escape viscous drag? *Rev. Fish Biol. Fish.* **6:** 353–360.

Müller, U. K., E. J. Stamhuis, and J. J. Videler. 2000. Hydrodynamics of unsteady fish swimming and the effects of body size: comparing the flow fields of fish larvae and adults. *J. Exp. Biol.* **203:** 193–206.

O'Dor, R. K. 1988a. The forces acting on swimming squid. *J. Exp. Biol.* **137:** 421–442.

O'Dor, R. K. 1988b. The energetic limits on squid distributions. *Malacologia* **29:** 113–119.

O'Dor, R. K., and J. A. Hoar. 2000. Does geometry limit squid growth? *ICES J. Mar. Sci.* **57:** 8–14.

O'Dor, R. K., and D. M. Webber. 1986. The constraints on cephalopods: why squid aren't fish. *Can. J. Zool.* **64:** 1591–1605.

Osse, J. W. M. 1990. Form changes in fish larvae in relation to changing demands of function. *Neth. J. Zool.* **40:** 362–385.

Packard, A. 1969. Jet propulsion and the giant fibre response of *Loligo*. *Nature* **221:** 875–877.

Preuss, T., Z. N. Lebaric, and W. F. Gilly. 1997. Post-hatching development of circular mantle muscles in the squid *Loligo opalescens*. *Biol. Bull.* **192:** 375–387.

Schmidt-Nielsen, K. 1997. *Animal Physiology. Adaptation and Environment.* 5th ed. Cambridge University Press, Cambridge.

Segawa, S. 1987. Life history of the oval squid, *Sepioteuthis lessoniana* in Kominato and adjacent waters central Honshu, Japan. *J. Tokyo Univ. Fish.* **74:** 67–105.

Svetlichnyy, L. S., and A. S. Svetlichnyy. 1986. Measurement of the locomotion characteristics of copepods attached to a dynamometer sensor. *Oceanology* **26:** 646–647.

Thompson, J. T., and W. M. Kier. 2001a. Ontogenetic changes in mantle kinematics during escape-jet locomotion in the oval squid, *Sepioteuthis lessoniana* Lesson, 1830. *Biol. Bull.* **201:** 154–166.

Thompson, J. T., and W. M. Kier. 2001b. Ontogenetic changes in fibrous connective tissue organization in the oval squid, *Sepioteuthis lessoniana* Lesson, 1830. *Biol. Bull.* **201:** 136–153.

Vogel, S. 1994. *Life in Moving Fluids.* 2nd ed. Princeton University Press, Princeton.

Webb, P. W., and D. Weihs. 1986. Functional locomotor morphology of early life history stages of fishes. *Trans. Am. Fish. Soc.* **115:** 115–127.

Weihs, D. 1974. Energetic advantages of burst swimming of fish. *J. Theor. Biol.* **48:** 215–229.

Williams, T. A. 1994. A model of rowing propulsion and the ontogeny of locomotion in *Artemia* larvae. *Biol. Bull.* **187:** 164–173.

Zar, J. H. 1996. *Biostatistical Analysis.* Prentice Hall, Upper Saddle River, NJ.

Zuev, G. V. 1966. Characteristic features of the structure of cephalopod molluscs associated with controlled movements. Ekologo-Morfologicheskie Issledovaniya Nektonnykh Zhivotnykh. Kiev, Special Publication. (Canadian Fisheries and Marine Services Translation series 1011, 1968).

Appendix

Description of the two force transducers used to measure the thrust produced by tethered squid.

Transducer 1

Force transducer 1 consisted of two brass blade elements (152 mm long, 6.4 mm wide, 0.25 mm thick) arranged at a right angle (*i.e.*, a cross) and attached to a 150-mm by 150-mm by 25-mm aluminum base (Fig. 1A). A hole drilled in the center of each blade element permitted insertion of a 10-mm length of 3.4-mm diameter threaded brass rod. The center of the threaded rod was drilled to accept the stainless steel post of the tether, which was glued in place using waterproof contact cement. The threaded rod was inserted through each blade element and held firmly by a brass nut on either side of the blade elements (Fig. 1A). The nuts also held the blade elements together tightly.

The tip of each blade element was clamped to the aluminum base. Slots were milled in the base to prevent the blade elements from contacting the base when deformed.

Four thin foil strain gauges (model CEA-13-250UW-350, The Measurement Group, Wendell, NC) were attached near the end of each blade element (*i.e.*, where the blade element was clamped to the aluminum base) and wired as a full Wheatstone bridge (see Biewener and Full, 1992). The strain gauges were waterproofed with several coats of silicone aquarium sealant.

The perpendicular arrangement of the blade elements permitted the magnitude of the thrust vector to be calculated using the Pythagorean theorem

$$F_T = \sqrt{(B_1^2 + B_2^2)}, \qquad \text{(Eq. 5)}$$

where F_T is the magnitude of the thrust vector, B_1 is the output of bridge 1, and B_2 is the output of bridge 2.

Transducer 2

Force transducer 2 consisted of a single aluminum blade element (57 mm long by 18 mm wide by 1.6 mm thick) screwed securely to a length of 26-mm by 26-mm steel box beam (Fig. 1B). The box beam was bolted to a steel frame positioned over the experimental arena.

A small aluminum block, which had been drilled to accept the stainless steel post of the tether, was screwed to the distal end of the blade element (Fig. 1B). A setscrew in the block held the post in place. The post extended 40 mm beyond the end of the blade element.

Two semiconductor strain gauges (model ESU-025-1000, Entran Sensors, Fairfield, NJ) were attached near the base of the blade element (Fig. 1B) and wired as a half Wheatstone bridge.